New Fowler-Nordheim Injection, Charge Neutralization, and Gamma Tests on the REM RFT300 RADFET Dosimeter

J. Lipovetzky, *Member, IEEE*, A. Holmes Siedle, *Senior Member, IEEE*, M. García Inza, *Member, IEEE*, S. Carbonetto, E. Redin, and A. Faigon

***Abstract*—Through the injection of a Fowler-Nordheim tunnel current or the inversion of oxide fields during irradiation (Radiation-Induced Charge Neutralization), the oxide charge trapped in thick-oxide (300 nm) commercial RADFETs, often called Q_{OT} could be erased. Novel trapped-hole and interface characteristics were observed after treatments of this type at high doses. With both erasure techniques, it was possible only to neutralize a fraction of the oxide trapped charge. A non negligible amount of charge and border traps is deemed here to be "intractable". That adjective an a symbol, Q_{IN}, are introduced for the first time in this paper. Later sections discuss the possible impact of these results. The conclusion for dosimetry is that a "reusable RADFET" dosimeter, working up to an unprecedented dose before wearing out, may be a practical possibility.**

***Index Terms*—Bias-controlled cycled measurements, dosimeters, Fowler-Nordheim tunnel injection, MOS devices, RADFET, radiation effects, REM RFT300, solid- state detectors.**

I. Introduction

THE working life of MOS dosimeters [1] normally ends when trapped charge in the dosimetric gate oxide approaches saturation, or when the shift in the threshold voltage (V_T) becomes so high that "reading" it becomes impractical. In recent years, two methods have been proposed for "resetting" or "erasing" MOS dosimeters, thereby extending working life. The first method consists of the electrical erasure by means of the injection of a Fowler-Nordheim (F-N) tunneling current in the oxide [2]. The injected electrons neutralize much of the positive oxide trapped charge as a result of a dynamic balance between trapping of electrons and trap ionization. The second method [3], [4] takes advantage of the effect known as Radiation Induced Charge Neutralization (RICN), first reported by Poch *et al.* [5] and fully modeled by Fleetwood [6]. If during irradiation the gate voltage is switched from a positive to a zero or negative value, the inversion of the electric field in the oxide changes the direction of drift of radiation-generated holes and electrons, bringing electrons towards the Si-SiO_2 interface where they can neutralize previously trapped holes. These two techniques were developed and applied in thin thermal oxides and floating gate transistors [2]–[4], [7]—thickness from 25 to 70 nm. One of the present authors (AH-S) suggested the extension of the method to thicker oxides. There was no guarantee that the high gate voltages required for such an experiment—five to ten times higher than previous experiments—, could be controlled without destroying or severely stressing the silica gate-oxide. The extra oxide thickness could also be regarded as new "real estate" for the formation of trap sheets of an interesting new kind. As will be described, there was also the attractive practical possibility of using Bias-Controlled Cycled Measurements (BCCM) [5] to extend the dose range of this dosimeter and hence its applications.

Section II describes the RADFETs used in this work and experimental details. Section III presents the results of F-N injection and irradiation. Section IV presents the results of new departures in RICN on the devices with high doses of ^{60}Co gamma rays. Section V discusses the results and the possible impact of the work in dosimetry, and Section VI presents conclusions.

II. Description of Samples and Experimental Details

The "erasure" methods described above are applied here for first time to a well-established MOSFET dosimeter. The REM RFT300 [8], gate oxide 300 nm, is a RADFET dosimeter with an oxide grown specially to give sensitivity matched to space and radiotherapy dosimetry, with a proven dose resolution of 1 rad (1 cGy). The dose which can be measured in the normal bias modes [8] ranges from rads to hundreds of krads. The RFT300 die comprises two transistors, Q1 and Q2, with a gate area of 7500 μm^2, a capacitor C with an area of 50 000 μm^2, and a p-n photodiode, the last two structures being mainly for diagnostic purposes. Dosimetric use requires a minimum of five leads. The masses surrounding the sensor chip are made as low as possible and are of low atomic weight. The carrier plugs into a commercial 6-way socket system for flat flexible cables. The carrier is easily drilled or trimmed, can be modified to be windowless ("zero overburden") and is frequently soldered or glued to the

Manuscript received July 10, 2012; revised September 17, 2012; accepted September 18, 2012. Date of current version December 11, 2012. This work was supported by ANPCyT and UBA by the grants PICT Redes 2007 1907, UBACyT I096, and REM Oxford Ltd. The works of M. García Inza and S. Carbonetto were supported by Peruilh grants.

J. Lipovetzky and A. Faigon are with the Device Physics-Microelectronics Lab., INTECIN, Facultad de Ingeniera, Universidad de Buenos Aires, C1063ACV, Ciudad de Buenos Aires, Argentina, and also with the Consejo Nacional de Investigaciones Científicas y Técnicas (CONICET), Buenos Aires, Argentina (e-mail: jose.lipovetzky@ieee.org; afaigon@fi.uba.ar).

A. Holmes-Siedle is with REM Oxford Ltd., Witney, OX29 4PD, U.K. (e-mail: ahs@radfet.com).

M. García Inza, S. Carbonetto, and G. Redin are with the Device Physics-Microelectronics Lab., INTECIN, Facultad de Ingeniera, Universidad de Buenos Aires, C1063ACV, Ciudad de Buenos Aires, Argentina (e-mail: magarcia@fi.uba.ar.; scarbonetto@fi.uba.ar; eredin@fi.uba.ar).

Color versions of one or more of the figures in this paper are available online at http://ieeexplore.ieee.org.

Digital Object Identifier 10.1109/TNS.2012.2222667

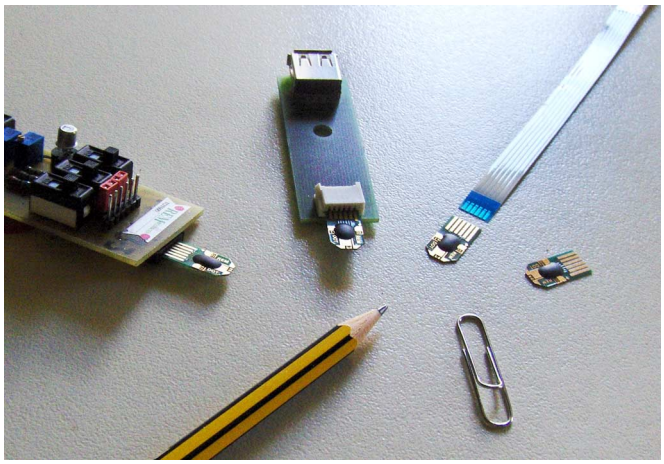

Fig. 1. REM RFT300 RADFETs showing possible connection modes and the geometry of the chip carrier (6 × 1.25 mm pads and epoxy chip covering). In the centre of the figure, a socket used by Frohlich *et al.* [29] is shown, as used to mount an array of RADFETs on magnets of the ELETTRA X-ray laser. On the left is a small REM circuit reader module which supplies switching and biasing for "read" and "expose bias" modes. A standard FFC ribbon connection is shown on the right [10].

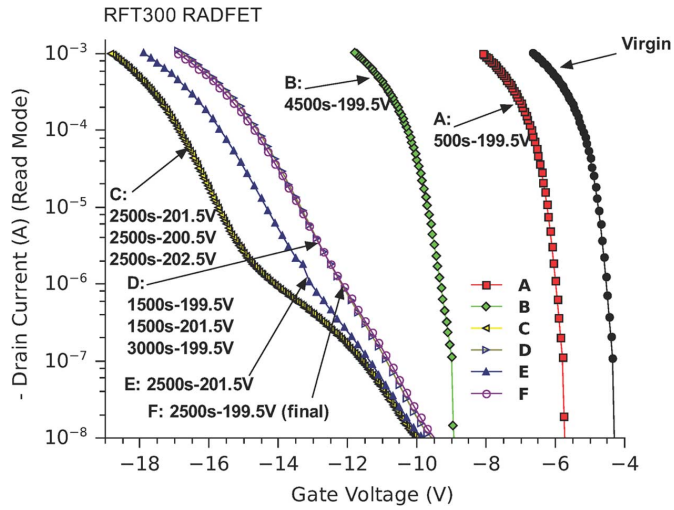

Fig. 2. F-N INJECTION ONLY; I-V curves after injection steps increasing first the stress time and then the positive gate voltage.

outside of a spacecraft to detect low-energy particle doses. In the present work, the presence of two simple identical devices side by side allowed an interesting controlled comparison of F-N and gamma excitations. The response of this die has been characterized under many different conditions [9]. Fig. 1 shows a photograph of REM RFT300 RADFETs in their package [10].

In this paper, the following conditions, symbols and abbreviations will apply. Doses will be expressed in rad(SiO_2) (1 cGy = 1 rad). ^{60}Co irradiations were at rates between 6 and 610 rad/s. A "bout of gamma" or "irradiation" implies exposure of the RADFET to gamma rays under bias during a fixed amount of time. A "bout of F-N" of "F-N stress" implies electron injection from Si by F-N tunneling under bias during a fixed amount of time. Recovery of V_T by the use of gamma under a low negative or zero gate voltage is known as RICN. The voltage used in this process is known as the RICN voltage, $V_{\rm RICN}$ corresponding to oxide field $E_{\rm RICN}$. The use of radiation to build up trapped charge is known as positive-charge buildup (PCB) and the gate voltage employed is here called $V_{\rm PCB}$ with an oxide field $E_{\rm PCB}$. The corresponding responsivity values for gamma responses are $r_{\rm RICN}$ and $r_{\rm PCB}$. We will consider the threshold voltage (V_T) as the one applied from gate to source (gate and drain shorted), to sustain a reference constant drain current $I_{\rm REF}$. When possible, we used $I_{\rm REF} = -490$ μA which is the nominal Zero Temperature Current (ZTC) of the RFT300 [8].

III. Fowler Nordheim Injection Experiments

Gate voltages in the neighborhood of +200 V were applied, one FET at a time, to an RFT300 RADFET (D, S and other leads grounded). This gave a controlled electron injection current by F-N tunneling from the silicon into the oxide [11]. No evidence of oxide breakdown, nor significant growth of later gate leakage, was seen in the transistors. This was made possible by carefully limiting gate current below 300 pA (i.e., current density below 4 μA/cm^2). The minimum F-N gate voltage $V_{\rm FN}$ giving observable I-V or C-V effects was 199.5 V. Experiments with the capacitor C gave similar responses to FETs but the latter yielded better results, probably because of the much smaller gate area. As mentioned above, the injection of one MOSFET did not affect the other, allowing comparisons of gamma ray effects before and after F-N injection. Over 80 controlled injection bouts were performed without detectable oxide breakdown, although interface state concentration built up steadily.

A. Effect of F-N Injection on the RADFETs and Repeatability

The effects of F-N stress on one FET are shown in Fig. 2, where I-V curves after several bouts of F-N stress are plotted. For virgin FETs, a constant gate voltage of 199.5 V, applied for 5 000 seconds, caused an increase in the positive oxide trapped charge. The virgin curve moves to curve A then to B. A small increase in interface trap density $(D_{\rm IT})$ is observed as a stretchout of the I-V curves [12]. Higher voltages—up to 202.5 V—, then yielded a further increase in oxide trapped charge and interface traps—see curve C. The explanation of this counter-intuitive result—electrons injection generating positive trapped charge—, will be given later. Further F-N using a voltage of 199.5 V reduced positive charge (curve D). Applying a higher voltage of 201.5 V increased it in 1 V (curve E). The superposition of curves D and F in Fig. 2 suggest that a repetitive cycle of charge and discharge may be set up. In [2], a repeatable cycle of this kind was set up in a thinner dosimetric oxide and, in [11], similar stress cycles for data storage in oxides were demonstrated.

Fig. 3 shows the same measurements, but tracking V_T ($I_{\rm REF} = -490$ μA), and interface trapped charge $(\Delta D_{\rm IT})$ [13] after each 500 second bout of injection. The virgin values near −5 V could not be restored. After an initial rapid rise in V_T from −5 V to −16 V, the value then fluctuates between −18 V and −16 V. We see here an initial indication that an F-N induced cycle of V_T values can be controlled by raising and lowering $V_{\rm FN}$. We later demonstrate that this "reset process" has uses in ionizing-radiation dosimetry. However, the cycling does not produce a return to the initial virgin V_T. Some of the

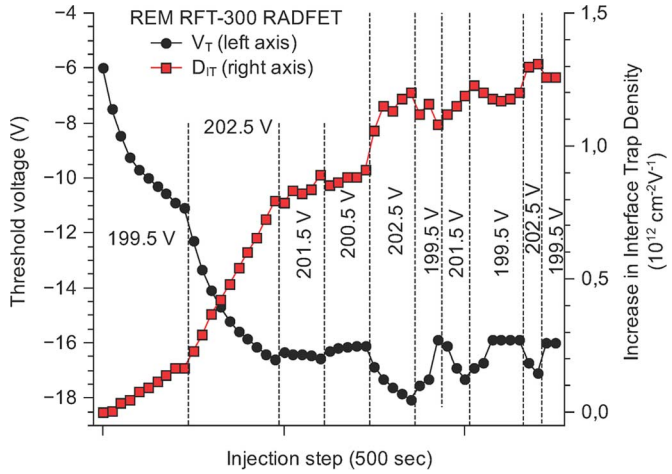

Fig. 3. F-N INJECTION ONLY; Same experiment of Fig. 2, following the evolution of V_T (490 uA) and interface trapped charge every 500 seconds.

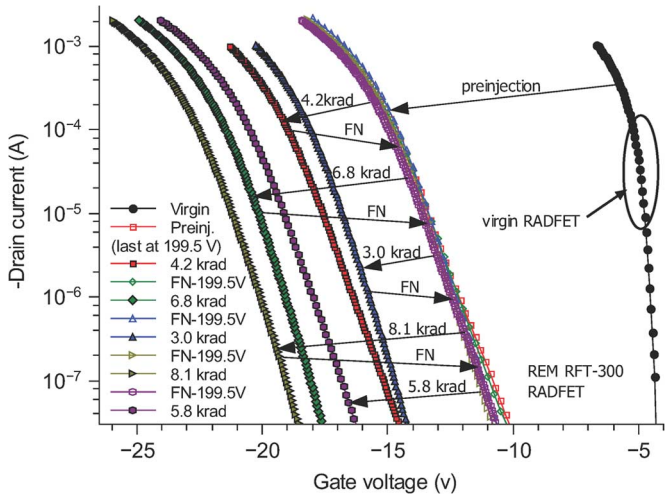

Fig. 4. F-N INJECTION FOLLOWED BY GAMMA IRRADIATION Drain current vs. gate voltage in FET Q1 after five irradiation and F-N reset cycles.

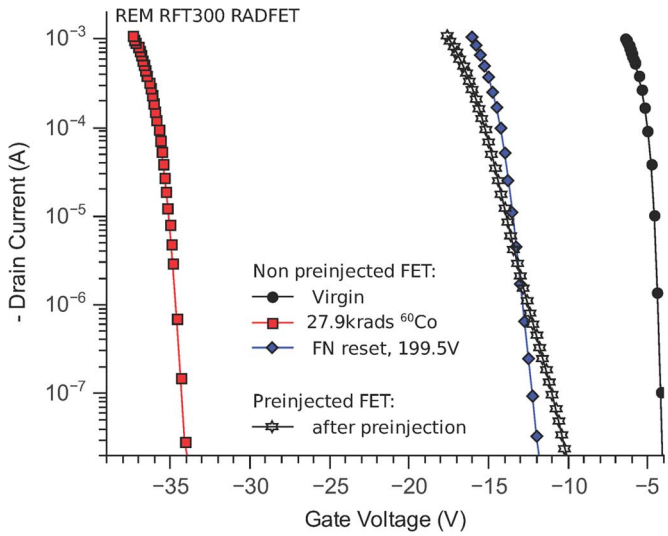

Fig. 5. GAMMA IRRADIATION FOLLOWED BY F-N INJECTION Drain current vs. voltage curves in FET Q2, showing neutralization of radiation-induced trapped holes by injected electrons.

injected charge is resettable but there is a fraction which is not, i.e., there is an "intractable" residue. The $D_{\rm IT}$ measurements in Fig. 3 and the way that they follow the V_T cycles point to a strong relation between the F-N-induced charge in the oxide and in the interface.

One refinement which was adopted during later resets came about because of the lowering of the F-N barrier at high V_T values. This made difficult to control the F-N current making dielectric breakdown more likely. It was found that the problem was eased if $V_{\rm FN}$ was ramped up gradually.

B. Irradiation and Reset

Then, the RADFET was irradiated several times. After each irradiation, the FET Q1 was reset applying bouts of F-N injection at $V_{\rm FN} = 199.5$ V, which is a $V_{\rm FN}$ value established above to bring V_T close to -16 V. F-N injections were done after irradiation. A ^{60}Co gamma source, at dose rates from 7 to 15 rads/sec delivered bouts of dose from 3.0 krad to 8.1 krad under a gate bias $V_{\rm PCB} = +9$ V in both FETs, with all other leads grounded.

Fig. 4 shows the I-V curves after each bout of gamma and F-N. Bouts of gamma rays produced trapped $Q_{\rm OT}$ [15] with its corresponding shift towards the left in the curves. It can be seen that then, F-N reset restored the I-V curves towards the right to similar positions, and V_T to a value close to (-16.0 ± 0.3) V (at -490 μA). To allow for initial (room temperature) post F-N anneal, plotted I-V curves were measured at least one day after injection. Much less fading occurred after irradiation but the same one-day delay was applied.

In the above F-N experiments (Figs. 2 and 3), the second transistor on the same die, Q2, had not been F-N preinjected, and during gamma bouts the same $V_{\rm PCB} = +9$ V, a standard value for the RFT300 was applied.

The responsivity r of "preinjected" Q1 was lower than the "non-preinjected" Q2. The figures were for Q1 $r = 1.25$ mV/rad and for Q2, $r = 0.95 + 0.05$ mV/rad, a drop of 24%. This may be because F-N charges had disturbed internal field profiles causing partial "field collapse" [16], [18]. This leads to a decrease in the gamma-induced hole generation [15]. The density of interface traps estimated from the subthreshold slope of the curves did not increase significantly after the five irradiation-reset cycles in the preinjected Q1.

During the five irradiation bouts the transistor Q2, was given 27.9 krads—see the shifted I-V curve plotted Fig. 5. After that, three F-N bouts of 500s at 199.5 V and a day of anneal at room temperature brought the curve to a stable position, as shown. Through this partial erasure of trapped charge, the threshold voltage could be restored only to -15.2 V (at $I_{\rm REF} = -490$ μA), a value similar for preinjected Q1. Also, it can be observed that the amount of interface traps is lower in the non preinjected Q2 with $\Delta D_{\rm IT} = 3.6 \cdot 10^{11}$ cm^{-2}eV^{-1}.

In summary, F-N erasure always restored V_T to ~ -16.0 V (-490 μA) in the preinjected Q1, and ~ -15.2 V (-490 μA) in the non-preinjected Q2. This was the same level at which preinjection yields a repeatable reset value of V_T, not again the "virgin" V_T of -5.5 V (-490 μA). Since a method for annealing the residual charge has not been found to date, it will here be described as "intractable charge".

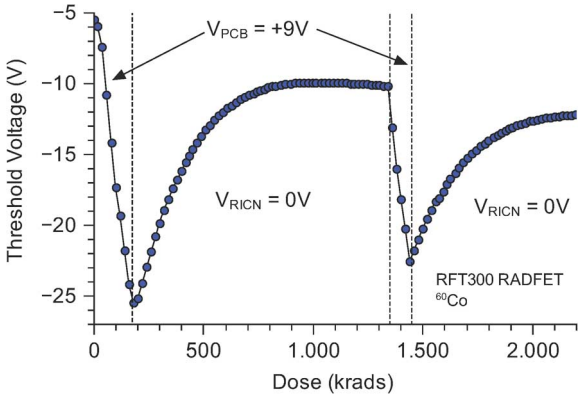

Fig. 6. GAMMA ONLY +9 AND 0 V—Two cycles radiation-induced charge generation (PCB) and neutralization (RICN) at V_G (irradiation) =+9 V and 0 V. V_T was tracked with $I_{\rm REF} = -490\ \mu$A.

IV. Radiation Induced Charge Neutralization (RICN) Experiments

To characterize the response of a dosimeter at different values of gate biases, a virgin RADFET was exposed to a much higher dose rate, 610 rads/sec. Most of the time the FET Q1 was in the "exposure mode" ($V_{\rm PCB}$ on the gate, all other leads grounded). Every five seconds, and during less than 70 ms, the RADFET was switched to the "read mode" measuring V_T. The switching between "expose" and "read" mode was automatic [7]. Measurements of V_T were repeated every few seconds (every 20 krads, approx.). During this test, the FET Q2 remained with all its leads grounded (nominally, $V_B = 0$, although a work function difference persists between Al and Si producing a voltage drop across the oxide of -0.5 V). During this first experiment, about 15 cycles were carried out between $V_{\rm PCB} = +9$ V and zero. The first two cycles are shown in Fig. 6 and the following in Fig. 7. Fig. 6 shows the evolution of V_T during irradiation, where initially a $V_{\rm PCB}$ of +9 V was used. When V_T reached -25 V ($-490\ \mu$A), the gate bias was switched to zero volts. As a result of the change in V_G, V_T recovered to a near-steady level of ~ -10 V ($-490\ \mu$A). A new switch of V_G to +9 V followed by 0 V brings V_T to a lower steady value. However, a slow negative drift after reaching the steady levels, due to border traps, made close comparisons difficult. Fig. 7 shows the continuation of cycling between +9 and zero volts, the only minor difference being a change in the "read" current to $-40\ \mu$A, in order to avoid V_T values reaching the limit of the V_T tracker (-25 V). In the figure, we see an identical cycling pattern but a new feature develops decreasing steady levels for the rest value of V_T.

A. RICN Under Different Gate Bias

The next experiment was to find the dependence of recovery rate on the gate voltage during recovery. We term the recovery phase "RICN" [3], [6]. With the same device constantly under irradiation at 610 rads/sec the effect of varying $V_{\rm RICN}$ was studied as follows. V_T was shifted to -24 V under $V_{\rm PCB} = +9$ V, and various $V_{\rm RICN}$ values, from zero to -10 V were applied. Results are shown in Fig. 8. Even small negative values of $V_{\rm RICN}$ enhanced the rate of RICN. The maximum initial rate was at $V_{\rm RICN} = -6$ V. The maximum amplitude,

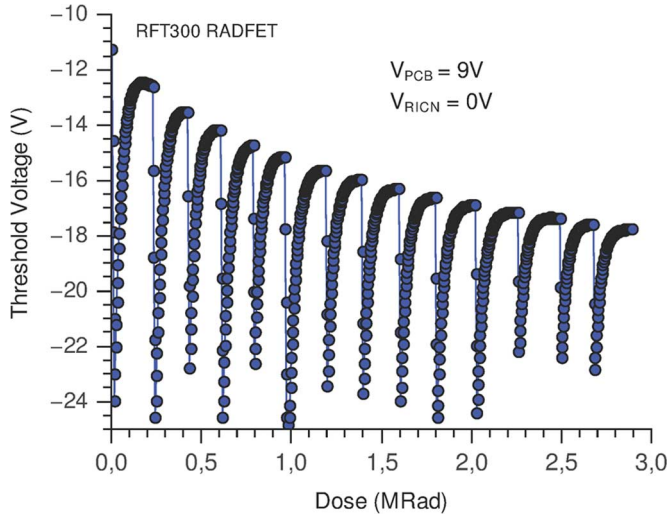

Fig. 7. REPEATED GAMMA AND RICN. V_T variations during repeated irradiations at V_G (irradiation) =+9 and 0 V. The 0 V phase shows a characteristic "recovery pattern" which saturates at decreasing voltages during the first megarads. V_T was tracked with $I_{\rm REF} = -40\ \mu$A.

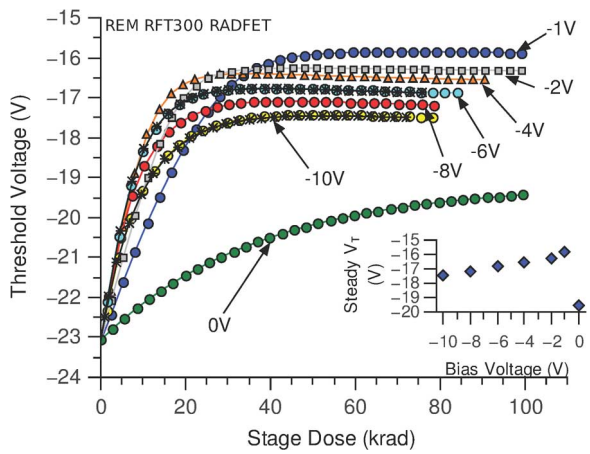

Fig. 8. MANIPULATING RICN FIELD. Charge buildup (PCB) and RICN patterns (gamma rays only) for various neutralization voltages. The curves here show the evolution of V_T under RICN at various values of V_G during stress. RICN responses at $V_{\rm RICN} = -6$ V and $V_{\rm RICN} = -10$ V were measured twice. Recovery responses overlap, showing their repeatability. The inset shows the saturation values of V_T at the different RICN voltages. Each RICN recovery stage requires about 100 krad. V_T was tracked with $I_{\rm REF} = -40\ \mu$A.

bringing V_T ($-40\ \mu$A) to about -16 V was at $V_{\rm RICN} = -6$ V. Note that this is, still well above virgin V_T value, but shows that RICN yields reset effects similar to those of F-N injection ($V_T \simeq 14$ V at $-40\ \mu$A). The change with $V_{\rm RICN}$, of RICN rate will be discussed in Section V.

B. Bias Controlled Cycled Measurements

A technique named Bias Controlled Cycled Measurement (BCCM) was proposed in 2008 [3]. BCCM consists on alternating periods of PCB and RICN, constraining V_T to move within a prescribed window. The window is chosen in a range in which the responses in both periods are linear with dose and yield relatively high responsivities. This means that they must lie well away from a charge-saturation condition. Using BCCM, we can usefully perform dosimetry by extracting a dose value from either the "up" or "down" period in these "triangular" traces. This then greatly increases dose range—it

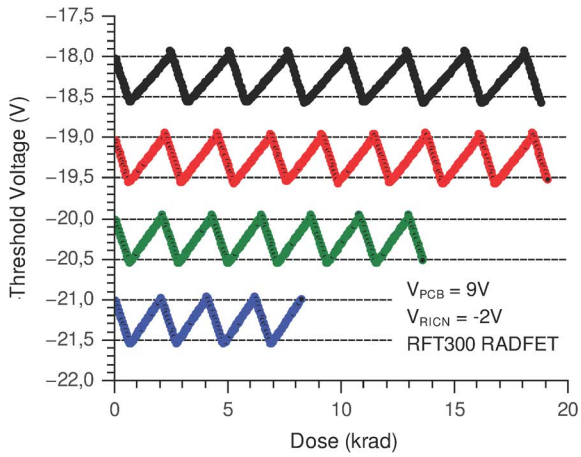

Fig. 9. RECOVERY PATTERNS WITH MAINTAINED V_T VALUES. A technique known as BCCM in which V_T is cycled between preselected values—see text. V_T was tracked with $I_{\mathrm{REF}} = -40\ \mu$A.

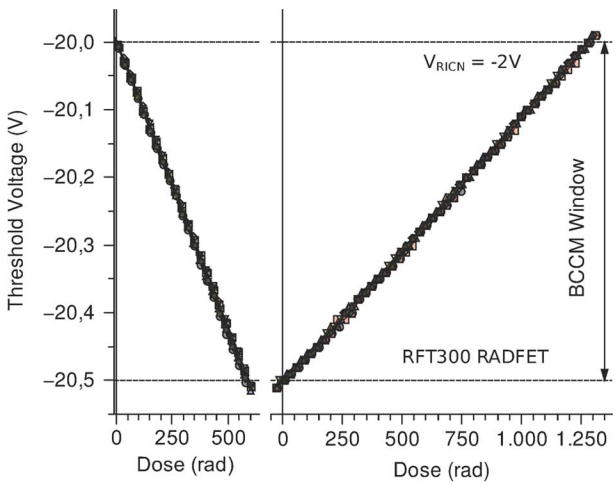

Fig. 10. CALIBRATION OF A BCCM PATTERN. Cycling a device between $V_T = 20.0$ and 20.5 V in steps of about 25 rad demonstrates the linearity offered by the BCCM method, The +9 V responsivity (left hand curve) is about 0.8 mV per rad. This is about twice that for the recovery curve to the right. This is suitable for a dosimetric calibration.

was reported an increase of at least one thousand times—and also permits the use of a voltage-measuring instrument of limited range e.g., a 24-bit A/D converter.

In the BCCM experiment, the FET of Figs. 6 to 8 was then irradiated at a rate of 5.6 rads/s. The threshold voltage sweep was limited to 0.5 V, somewhere between −21.5 V and −18.0 V, and the bias voltages used were $\mathrm{V_{PCB}} = +9$ V, and $V_{\mathrm{RICN}} = -2$ V. Fig. 9 shows a selection of such sweeps spread over that range.

The calibration of one such sweep is shown in Fig. 10. V_T of a heavily-irradiated RFT300 was cycled between −20.0 V and −20.5 V in steps of about 20 krad. The response curves, demonstrate the linearity of dose response offered in both the "up" and the "down" parts of the cycle. The +9 V responsivity r_{PCB} (left hand curve) is 0.86 mV/rad. This is about twice the value of r_{RICN}, which is 0.39 mV/rad. Such responses can be calibrated to a few percent dosimetric accuracy despite heavy accumulated dose values for the device.

V. Discussion

Ever since it was realized that MOSFET devices would exhibit positive-charge buildup (PCB) in the insulator under the gate, a physical model for this effect has been based on the slow transport of holes, if driven by a field of the order of 100 V/μm, to a pre-existing trap sheet in a strained region located quite near to the Si-SiO_2 interface. The new, positive oxide trapped charge, ΔQ_{OT}, shifts the threshold voltage by a corresponding amount ΔV_T.

Even in thick oxides, moderate amounts of Q_{OT} can be completely discharged by photoemission of electrons from the silicon using UV light. It is possible that such a clear erasure picture would still occur for similar photoemission into the heavy mount of charge existing in heavily irradiated or injected samples of thick oxides such as in the present experiment.

A. Reset of Oxide Charge by F-N Injection

We found that F-N removed the additional gamma-induced Q_{OT} in a so-called "preinjected" FET (see Fig. 4). By contrast, only a fraction of the same charge in a virgin device was removed but leading V_T to the same steady value (see Fig. 5). The gamma responsivity of a F-N injected sensor was also depressed. There is a similar partial removal of Q_{OT} by RICN (Figs. 6 to 8). The latter finding on the resetting power of F-N and RICN is similar to findings for thinner oxides in [2] and [3].

In the present experiments the removal of F-N induced charge has never been complete, using either F-N at reduced $V_{\mathrm{F\text{-}N}}$ or RICN. This suggests that "intractable trapped charge", which we here name "Q_{IN}" is trapped in locations or energy levels different from Q_{OT}. After "intractable charge" reaches a saturation state value, through long irradiation or charge injection, gamma responses became repeatable. F-N injection at 202.5 V (see curve C of Fig. 2) gives saturation in a short time, whereas the saturation of Q_{IN} under gamma irradiation bias required a long time and 8 Mrads.

The gamma responsivity of a RADFET saturated in this way by F-N stressed Q1 decreased by 24% and V_T shifted by about −10 V due to Q_{IN}. A transistor on the same die which had not had F-N injection had responsivity depressed by only 6% after the same V_T shift (this is a moderate and expected "field collapse").

These findings suggest that the intractable charge is separate in both energy and location from Q_{OT}. For discussion, we postulate separate sheets of charge in the oxide, Q_{OT} and Q_{IN}. One possibility is that Q_{IN} is formed by a combination of interface traps and "deep" border traps [22], having a high rate of creation during the first few krads of irradiation. Considering the extensive oxide region between the normal Q_{OT} region and the gate, thick oxides present greater scope for accommodating intractable charges than thin oxides. The I-V curves of Fig. 3 demonstrate a decrease in the sub-V_T slope, indicating that injection of electrons from the silicon generate both positive Q_{OT} and other charge in the border or interface region. In [25], different energy-levels of interface-traps were reported for different kinds of injection, a finding which might be applicable to the present results. Nissan-Cohen *et al.* [11] conclude that in such cases, the creation of positive charge can be accounted for by impact ionization.

A slight dependence of the steady V_T voltage with F-N injection voltage is observed in Fig. 3. This dependence can be the result of two competing mechanisms—the neutralization of trapped holes by injected electrons, and the trapping of holes generated by impact ionization or anode hole injection [11], [22]. A small increase in the oxide field may cause an important increase in the generation of holes, which alters electron-hole equilibria to give higher positive trapped charge [14], [23].

In our experiments, high voltage F-N injection was not carried out during irradiation. However, in a low dose environment, e.g., in space applications, there is no reason why concurrent exposure and F-N injection should differ much from the same processes done separately.

B. Reset of Oxide Charge by RICN

The RICN rates in Fig. 8 show a dependence on $V_{\rm RICN}$ in their initial slopes and in their saturation levels. The maximum initial rate is at $V_{\rm RICN} = -6$ V. The largest recovery is at $V_{\rm RICN} = -1$ V.

These effects can be understood by considering how the applied electric field affects generation yield, transport of carriers, and trapping cross section. In the $V_{\rm PCB} = +9$ V stages in Figs. 5 to 9, $Q_{\rm OT}$ grows as a result of the known positive oxide charge buildup. The accepted picture is that, for high $E_{\rm PCB}$, nearly all the holes generated then escape recombination, move towards the substrate and get trapped in a sheet of oxide defects. the $Q_{\rm OT}$ region. The centroid of this region lies between 15 and 5 nm from the Si-SiO_2 interface.

However, when field direction is reversed, electrons from the bulk of the oxide drift towards the Si-SiO_2 interface. The $Q_{\rm OT}$ sheet is in their path, and some trapped holes are neutralized. This is the RICN effect [6]. For our purpose, this description is not adequate unless the local fields, the result of fields from local charges and the external bias, are considered using Gauss Law. The effect of PCB is well characterized in models, including the well known "field collapse" effect with its reduction in the radiation-induced e-h generation yield and hence in the dosimetric response. By contrast, in RICN conditions, the local field enhances the applied field. The field generated by $Q_{\rm OT}$ it will attract free electrons. This is why, even with $V_{\rm RICN} = 0$ V, the oxide trapped charge reduces in the observed response in Figs. 5 to 7.

In the context of low $V_{\rm RICN}$, the electric field dependence of the response during RICN is dominated by the generation yield. This represents the yield of electrons available for $Q_{\rm OT}$ neutralization. In Fig. 11, the blue square symbols represent the conversion of our data from Fig. 5 into the rate of detrapping of holes. These are taken from the slopes of the curves at $V_T = -22$ V. The units are the number of holes (per dose and unit area) which are being neutralized as a function of the external electric field. The $Q_{\rm OT}$ centroid is assumed to lie 10 nm form the Si-SiO_2 interface and $\Delta V_{\rm OT} = N_{\rm OT} \cdot q/C_{\rm OX}$ where $\Delta V_{\rm OT}$ is the contribution of oxide trapped charge to the V_T shift, $N_{\rm OT} = Q_{\rm OT}/q$, q the electron charge, and $C_{\rm OX}$ the capacitance per unit area of the oxide.

In the same plot, we show (as circles) the fluence of electrons per unit dose Jn which escape after e-h generation ($8.1 \cdot 10^{12}$ pairs·cm^{-3}·rad^{-1}), multiplied by the generation yield Y calculated for ^{60}Co irradiation as $Y = (0.55/E_{\rm OX} + 1)^{-0,7}$, where $E_{\rm OX}$ is the local electric field in the oxide (as before, $Q_{\rm OT}$ centroid 10 nm from the Si-SiO_2 interface) [15]. The internal field estimation takes in account the flatband voltage.

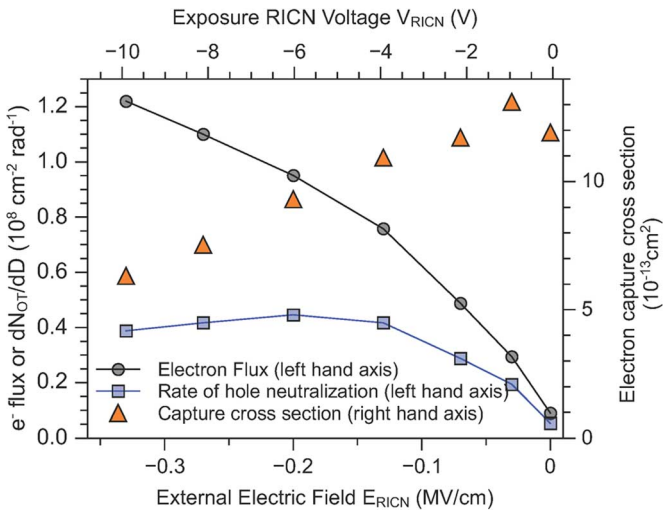

Fig. 11. MODELLING OF RICN RESPONSES. The state of the oxide and its traps at various fields during the low-voltage recovery stage. The dependence on field $E_{\rm RICN}$ of (a) the capture cross-section of holes for electrons, (b) the gamma-induced electron flux, (c) the resulting neutralizarion.

On this model, it can be concluded that, at low negative electric fields, half of the electrons generated in the oxide meet and neutralize a trapped hole. This blue squares curve shows a maximum at 0.2 MV/cm ($V_{\rm RICN} = -6$ V), but, as the absolute value of $V_{\rm RICN}$ increases further, say to 0.3 MV/cm (-9 V), the probability of neutralizing a trapped hole decreases to near 40%. The maximum field in our experiments was -0.33 MV/cm (-10 V). Assuming an initial density of trapped holes $N_{\rm OT} = 5 \cdot 10^{11}$ cm^{-2},—which derives from the 7 V reversible V_T shift of the responses shown in Fig. 8—, the cross section which electrons have for annihilation by a trapped hole $\sigma_{\rm RICN}$ was plotted, using that $dN_{\rm OT}/d_D = J_n \sigma_{\rm RICN} N_{\rm OT}$ (see red triangles).

The cross section $\sigma_{\rm RICN}$ falls as electric field rises. The dependence is a straight-line to the left side of the Fig. 11, say above 0.07 MV/cm ($V_{\rm RICN} < -2$ V). This is in agreement with a similar finding of Krantz [23] (also a low-field case), but different from the $E^{-3/2}$ dependence typical of electric fields in the range above 1 MV/cm [23], [24]. Perhaps this is because the capture cross section appears very sensitive to field in the lower regions, including a strong deviation from linearity between -2 V and 0 V.

A method of dosimetry employing the above RICN effects for large dose shots would be based on Fig. 10 (right-hand curve) and would involve monitoring the discharge of a suitable premeasured, amount of positive oxide charge generated by gamma rays.

After the premeasured amount of charge has been used up, the RADFET would be removed and sent for re-charging. From Fig. 11, we predict a maximum in responsivity $r_{\rm RICN}$ in this dosimetric discharge curve is obtained at $E_{\rm RICN} \simeq -0.2$ MV/cm. This maximum is a result of the increase in the generation yield with $E_{\rm OX}$, countered by a

corresponding rapid fast decrease in the capture cross section (Fig. 11). The fields at which maximum RICN responsivity are observed are, of course a fraction of an MV per cm. By contrast, PCB responsivity ($r_{\rm PCB}$) continues to increase up to at least 4 MV/cm (132 V for RFT300) [26], [27]. At higher fields, breakdown, avalanche and tunnelling effects may complicate the picture [9]. The maximum responsivity value in the RICN experiment was 0.62 mV/rad, lower than the responsivity observed in virgin RADFETs during PCB, which for with a +9 V bias exposure had in our experiments values of 0.95 mV/rad for a preinjected device, 0.86 mV/rad for the heavily irradiated device using BCCM, 1.25 mV/rad in a fresh RADFET a +9 V and 1.75 mV/rad for +18 V.

The saturation of Charge Neutralization with $V_{\rm RICN}$ in Fig. 8 inset is of interest. This is probably due to how the cross section of hole capture in neutral traps, and cross section of hole neutralization by electrons vary with field. In [23] it is postulated that the capture of holes by neutral traps decreases more slowly with field than the capture of electrons by positive traps. In Fig. 8, the "steady V_T" values plotted in the inset might come about if, as the field $E_{\rm RICN}$ increases, the trapping of a locally-generated hole exceeds that of its neutralization by an incoming electron.

Heavy irradiation is required to obtain repeatability under BCCM such as that shown in Figs. 9 and 10. "Heavy" implies a total dose of many megarads and interface- and border-trap concentrations of at least $1.6 \cdot 10^{12}$ eV^{-1}cm^{-2}, as determined by the sub-V_T characteristics. The high concentration of border states naturally produces significant drift in V_T readings. Future work will determine the impact of drift on dose measurement and whether circuit measures can correct this drift [9].

It was indicated that isochronal anneals to 300°C removed all but a few percent of gamma-induced V_T shift. In [28], there is residual damage. On the other hand, in lightly-irradiated MOSFETs, [29], 100 hours of annealing at 150°C achieved a complete recovery on a type of commercial MOS dosimeter, although responsivity was depressed thereby. Research is needed to correlate $Q_{\rm IT}$ with non-annealable residues $Q_{\rm IN}$. In MOS technology the physics of such non-annealable or fixed charges in oxides is not widely understood. What is clear is that, despite these complications of intractable charge, thick-oxide dosimetry, radiation-induced $Q_{\rm OT}$ charge can still be injected and removed from the RADFET oxides independently in a predictable way which can be calibrated against multi-megarad doses. We submit that a "reusable RADFET" dosimeter, working up to an unprecedent dose before wearing out is a practical possibility.

VI. Conclusion

The present work proved that it is possible to apply space-charge erasure techniques on well established thick oxide MOS dosimeters. Further research will allow us to make an assessment of dosimetric accuracy. The study of multiple resets of trapped positive charge in 300 nm RADFET oxides using Fowler-Nordheim injection and Radiation-Induced Charge Neutralizaton shows promise in dosimetry and is potentially rich in basic and applied discoveries in oxide-film structure and charge trapping processes. The appearance of "intractable" charge $Q_{\rm IN}$, in dosimetric oxides is POSSIBLY a novel feature of thick-oxide technology. The applicability of the Bias-Controlled Cycled Measurements technique of Faigon *et al.* has been extended to thick-oxide dosimeters such as the RFT300 RADFET. Used with this commercial dosimeter, it would add versatility the high-dose end to an oxide dosimeter already capable of resolving 0.01 Gy (1 rad), at present over 4 to 5 orders of magnitude in dose. A "reusable RADFET" dosimeter, working up to a very high dose before wearing out, is a practical possibility.

Acknowledgment

The authors want to thank to the Planta Semi Industrial de Irradiaciones, Comisión Nacional de Energía Atómica, and to the Roffo Hospital, for the access to irradiation facilities; to Eva Pawlak and Diana Feld for her help with dosimetry and use of radiation sources.

References

[1] A. G. Holmes-Siedle, "The space charge dosimeter—General principles of a new method of radiation dosimetry," *Nucl. Instrum. Meth.*, vol. 121, pp. 169–172, 1974.

[2] J. Lipovetzky, E. G. Redin, E. G. , and A. Faigon, "Electrically erasable metal-oxide-semiconductor dosimeters," *IEEE Trans. Nucl. Sci.*, vol. 54, no. 4, pp. 1244–1250, Aug. 2007.

[3] A. Faigon, J. Lipovetzky, E. G. Redin, and G. Krusczenski, "Extension of the measurement range of MOS dosimeters using radiation induced charge neutralization," *IEEE Trans. Nucl. Sci.*, vol. 55, no. 4, pp. 2141–2147, Aug. 2008.

[4] J. Lipovetzky, E. G. Redin, M. A. D. Inza, S. Carbonetto, and A. Faigon, "Reducing measurement uncertainties using bias cycled measurement in MOS dosimetry at different temperatures," *IEEE Trans. Nucl. Sci.*, vol. 57, no. 2, pp. 848–853, Apr. 2010.

[5] W. J. Poch and A. G. Holmes-Siedle, "Long-term effects of radiation on complementary MOS logic networks," *IEEE Trans. Nucl. Sci.*, vol. NS-17, no. 6, pp. 33–40, Dec. 1970.

[6] D. M. Fleetwood, "Radiation-induced charge neutralization and interface-trap buildup in metal-oxide-semiconductor devices," *J. Appl. Phys.*, vol. 67, no. 1, pp. 580–583, 1990.

[7] M. G. Inza, J. Lipovetzky, E. G. Redin, S. Carbonetto, and A. Faigon, "Floating gate PMOS dosimeters under bias controlled cycled measurement," *IEEE Trans. Nucl. Sci.*, vol. 58, no. 3, pp. 808–812, Jun. 2011.

[8] REM Oxford Ltd., Datasheet Type RFT-300-CC10G1 RADFET RFTDAT-CC10(REV B). Oxford, U.K., 2009 [Online]. Available: www.oxford.com, REM

[9] A. G. Holmes-Siedle, F. Ravotti, and M. Glaser, "The dosimetric performance of RADFETs in radiation test beams," in *Proc. IEEE NSREC07 Radiation Effects Data Workshop Rec.*, 2007, pp. 42–56.

[10] L. Frohlich, K. Casarin, E. Quai, A. Holmes-Siedle, and M. Severgnini, "Online monitoring of absorbed dose in undulator magnets with RADFET dosimeters at FERMI@Elettra," *Nucl. Instrum. Meth. Phys. A*, 2012 [Online]. Available: http://www.sciencedirect.com/science/article/pii/S0168900212013551, to be published

[11] Y. Nissan-Cohen, J. Shapphir, and D. Frohman-Bentchkowsky, "Dynamic model of trapping-detrapping ins SiO_2," *J. Appl. Phys.*, vol. 58, no. 6, pp. 2252–2261, 1985.

[12] T. R. Oldham and F. B. McLean, "Total ionizing effects in MOS oxides and devices," *IEEE Trans. Nucl. Sci.*, vol. 50, no. 3, pp. 483–499, Jun. 2003.

[13] D. M. Fleetwood, M. R. Shaneyfelt, and J. Schwank, "Estimating oxide-trap, interface-trap, and border-trap charge densities in MOS transistors," *Appl. Phys. Lett.*, vol. 64, p. 1965, 1994.

[14] E. Miranda, E. G. Redin, and A. Faigon, "Modeling of the IV characteristics of high-field stressed MOS structures using a Fowler-Nordheim-type tunnelling expression," *Microelectron. Reliab.*, vol. 42, no. 6, pp. 935–941, 2002.

[15] A. Holmes-Siedle and L. Adams, *Handbook of Radiation Effects*, 2nd ed. Oxford, U.K.: Oxford Univ. Press, 2002.

[16] M. Garcia Inza, J. Lipovetzky, E. Redin, S. Carbonetto, and A. Faigon, "Ionizing radiation response of floating gate devices under bias controlled cycled measurement," in *Conf. Rec. RADECS Radiation Effects Compon. Syst.*, Längenfeld, Austria, Sep. 20–24, 2010, Austrian Institute of Technology - University of Montpelier.

[17] H. R. Boesch, F. B. McLean, J. M. Bennedetto, and J. M. McGarrity, "Saturation of the threshold voltage shift in MOSFETs at high total dose," *IEEE Trans. Nucl. Sci.*, vol. NS-33, no. 3, pp. 1191–1197, Jun. 1986.

[18] A. Holmes-Siedle, P. Christensen, L. Adams, and C. Seifert, "Modelling CMOS radiation tolerance in the high-dose range," in *Proc. 3rd Eur. Conf. Radiation and its Effects on Compon. and Syst., RADECS*, 1995, pp. 183–190.

[19] A. G. Holmes-Siedle and L. Groombridge, "Hole traps in silicon dioxide: A comparison of population by x-rays and band-gap light," *Thin Solid Films*, vol. 27, pp. 165–170, 1975.

[20] A. G. Holmes-Siedle, I. Groombridge, C. Emms, and J. Bosnell, "Gamma and vacuum ultraviolet irradiations of ion-implanted SiO_2 for MOS dielectrics," *IEEE Trans. Nucl. Sci.*, vol. NS-21, no. 6, pp. 159–166, Dec. 1974.

[21] D. M. Fleetwood, T. L. Meisenheimer, and J. H. Scofield, "1/f noise and radiation effects in MOS devices," *IEEE Trans. Electron. Devices*, vol. 41, no. 11, pp. 1953–1964, Nov. 1994.

[22] J. D. Di Maria and Stathis, "Anode hole injection, defect generation, and breakdown in ultrathin silicon dioxide films," *J. Appl. Phys.*, vol. 89, pp. 5015–5024, 2001.

[23] R. J. Krantz, L. W. Aukerman, and T. C. Zietlow, "Applied field and total dose dependence of trapped charge buildup in MOS devices," *IEEE Trans. Nucl. Sci.*, vol. NS-34, no. 6, pp. 1196–1201, Dec. 1987.

[24] D. A. Buchanan, M. V. Fischetti, and D. J. DiMaria, "Coulombic and neutral trapping centers in silicon dioxide," *Phys. Rev.*, vol. 43, no. 2, pp. 1471–1486, 1991.

[25] F. Palumbo, A. Faigon, and G. Curro, "Electrical correlation of double-diffused metal-oxide-semiconductor transistors exposed to gamma photons, protons, and hot carriers," *IEEE Trans. Electron Devices*, vol. 58, no. 5, pp. 1476–1482, May 2011.

[26] H. E. Boesch, Jr., F. B. McLean, J. M. Benedetto, and J. M. McGarrity, "Saturation of threshold voltage shift in MOSFETs at high total dose," *IEEE Trans. Nucl. Sci.*, vol. NS-33, no. 6, pp. 1191–1197, Dec. 1986, 1986.

[27] A. G. Holmes-Siedle and L. Adams, "Dosimetric silica films: The influence of field on the capture of positive charge," *IEEE Trans. Nucl. Sci.*, vol. NS-30, no. 6, pp. 1975–1979, Dec. 1982.

[28] D. Verellen *et al.*, "An in-house developed resettable MOSFET dosimeter for radiotherapy," *Phys. Med. Biol.*, vol. 55, pp. N97–N109, 2010.

[29] A. Kelleher, N. McDonnell, B. O'Neill, W. Lane, and L. Adams, "Investigation into the re-use of PMOS dosimeters," *IEEE Trans. Nucl. Sci.*, vol. NS-41, no. 3, pp. 445–451, Jun. 1994.